IEEE Access
Multidisciplinary | Rapid Review | Open Access Journal

Received June 30, 2020, accepted July 12, 2020, date of publication July 28, 2020, date of current version August 7, 2020.

Digital Object Identifier 10.1109/ACCESS.2020.3012494

Real Time Non-Invasive Hemodynamic Assessment of Ventricular Tachycardia

TUDOR BESLEAGA[1], PIER D. LAMBIASE[1,2], ADAM J. GRAHAM[2], ANDREAS DEMOSTHENOUS[3], (Fellow, IEEE), AND MICHELE ORINI[1]

[1]Institute of Cardiovascular Science, University College London, London WC1E 6DD, U.K.
[2]Department of Electrophysiology, Barts Heart Centre, London EC1A 7BE, U.K.
[3]Department of Electronic and Electrical Engineering, University College London, London WC1E 7JE, U.K.

Corresponding author: Michele Orini (m.orini@ucl.ac.uk)

This work was supported in part by the University College London (UCL) and in part by Integrated Technologies Limited. The work of Michele Orini and Pier D. Lambiase were supported in part by the Medical Research Council under Grant MR/N025083/1.

ABSTRACT Hemodynamically unstable ventricular tachycardia (VT) is a critical cardiac arrhythmia associated with hemodynamic compromise that requires immediate cardioversion to prevent sudden cardiac death. Since unnecessary cardioverter defibrillators shocks damage the heart and increase the risk of mortality, the discrimination between unstable (i.e. requiring cardioversion) and stable (i.e. not requiring cardioversion) VT is of paramount importance. The aim of this study was to propose and assess non-invasive identification of hemodynamically unstable VT using photoplethysmography (PPG). Seventy-five (n = 75) episodes of VT were recorded in 14 patients undergoing invasive electrophysiological studies for VT catheter ablation. Invasive continuous arterial blood pressure (ABP), PPG and electrocardiogram (ECG) were simultaneously recorded. VTs were classified as unstable if during the first 10 seconds from onset, the mean ABP ($\overline{P_{VT}} < 60P_{VT}$) was $\overline{P_{VT}} < 60P_{VT} < 60$ mmHg or if P_{VT} dropped more than 30% with respect to a 10 seconds baseline (i.e. ratio $R_{ABP} < 0.70$). Five PPG morphological features were derived and compared to the heart rate from the ECG. PPG markers detected hemodynamically unstable VT with accuracy as high as 86% and were more accurate than the heart rate. The mean absolute slope was the best PPG parameter for classification of $\overline{P_{VT}} < 60P_{VT} < 60\overline{P_{VT}} < 60$ mmHg (AUC = 0.85, Sensitivity = 72%, Specificity = 86%) and $R_{ABP} < 0.70 R_{ABP} < 0.70$ (AUC = 0.90, Sensitivity = 83%, Specificity = 89%) and it was automatically selected in the best two-variables logistic regression, for which AUC = 0.94. In conclusion, PPG analysis can accurately identify haemodynamically unstable VTs and has potential to enable optimization of VT therapy and reduce unnecessary and harmful cardioversion shocks.

INDEX TERMS Assistive technology, biomedical signal processing, cardiology.

I. INTRODUCTION

Ventricular tachycardia (VT) is a critical arrhythmia that in some circumstances can become life threatening. The condition manifests itself through consecutive rapid contractions dissociated from normal sinus rhythm and it can dramatically reduce cardiac output. The degree of danger associated with VT depends on its impact on arterial blood pressure (ABP), i.e. on its haemodynamic stability. Hemodynamically unstable VT is associated with abrupt ABP loss that can prevent oxygen and nutrients from circulating, therefore threatening vital organs function. Contrary to hemodynamically stable VT, which does not dramatically impact ABP, unstable VT requires immediate cardioversion to prevent sudden cardiac death.

Implantable cardioverter defibrillators (ICD) are capable of stopping life-threatening ventricular arrhythmias by delivering electrical shocks to the heart and are becoming mainstream (hundreds of thousands are implanted every year worldwide). Although potentially life-saving, defibrillator shocks damage the heart and increase the risk of death [1]–[4]. Therefore, reducing the number of unnecessary ICD shocks by specifically targeting unstable VT is a critical aspect for improving VT patients' care. In current practice, ICDs are programmed to deliver a shock when the heart rate increases above a pre-determined threshold,

The associate editor coordinating the review of this manuscript and approving it for publication was Filbert Juwono.

without taking into consideration ABP. Automatic identification of unstable VT remains however challenging, as no fixed relationship exists between heart rate and ABP during VT [5].

The photoplethysmogram (PPG) is a non-invasive optical signal measured in many wearable devices capable of providing real-time cardiac and haemodynamic information. We therefore hypothesised that PPG could be used to enable detection of hemodynamically unstable VT. The methodology presented in this study uses PPG features recorded before and at the onset of VT to classify its hemodynamic response. While previous studies have focused on improving alarm detection (including cardiac arrhythmia) in intensive care using PPG data [6] and others have classified ventricular arrhythmias based on electrocardiographic (ECG) features [7], non-invasive identification of unstable VT by means of PPG is novel. We envisage this study as a first step towards a new approach with the potential of improving clinical management of millions of patients relying on ICD therapy to stop life-threatening VTs.

II. METHODS

A. DATA SETS AND PRE-PROCESSING

Twenty-two (n = 22) patients undergoing catheter ablation of VT in the Catheterization Lab were prospectively recruited at the Barts Heart Centre, London, UK. ECG, invasive arterial blood pressure and PPG were simultaneously measured with sampling frequency of 240 Hz (Mac-Lab System, General Electric). Fourteen (n = 14) patients, out of the 22, exhibited VT and were included in the study. Their background is presented in supplementary Table S.I. PPG was recorded from the middle finger of the left hand. Signals were exported bypassing the patient monitor auto-gain filters. ABP and PPG signals were filtered with a finite impulse response (FIR) low pass filter of 30 Hz cut-off frequency and order 120. A 100 Hz low pass filter was applied to the ECG waveform. Data were collected as part of a Barts Heart Centre ethically approved study of VT ablation and patients gave informed consent.

In some patients, ventricular pacing (cycle length equal to 423 ± 32 ms, range 410-870 ms) was established to induce VT and 4 patients were studied while in slow incessant monomorphic stable ventricular tachycardia.

B. DATA ANALYSIS

The onset of each VT was time-stamped (t_0) and invasive ABP, PPG and ECG were evaluated in 3 windows (see Fig. 1): (A) From 10 s before to the onset of VT ($T_0 : t_0 - 10s < t < t_0$); (B) From the onset of VT to 10 s after it ($T_{VT} : t_0 \leq t < t_0 + 10s$); (3) Earliest 10 second interval preceding the VT onset, t_0, showing either normal sinus rhythm or baseline atrial pacing (T_{SR}). This additional reference window was considered because in some cases T_0 presented irregular rhythm due to ectopics or standard pacing maneuvers utilized to induce VT.

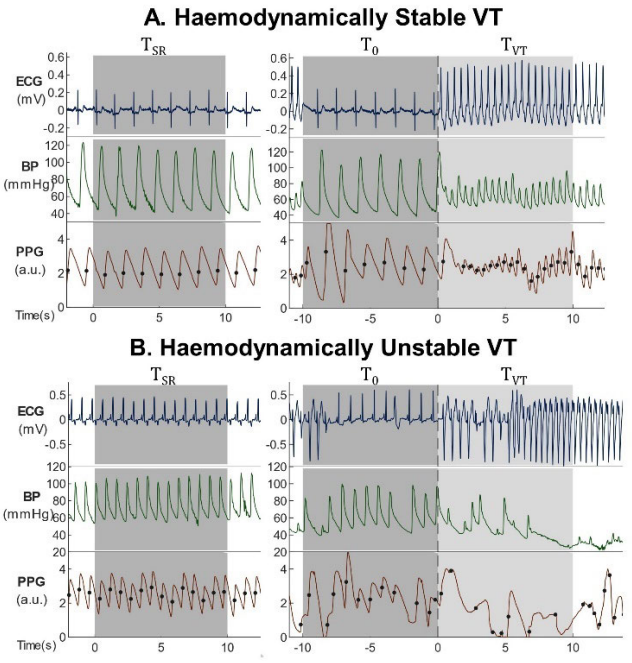

FIGURE 1. Recordings of ECG, invasive blood pressure (ABP) and non-invasive PPG during hemodynamically stable (A) and unstable (B) VTs, within 3 10-seconds windows: Sinus rhythm preceding VT (T_{SR}), any cardiac rhythm immediately before VT onset (T_0) and VT (T_{VT}).

1) ARTERIAL BLOOD PRESSURE AND DEFINITION OF UNSTABLE VT

Mean ABP was used to evaluate the hemodynamic response to VT. This is standard practice and more reliable than using measurements based on systolic blood pressure, since during fast VT it is not always possible to clearly distinguish blood pressure pulses. Hemodynamically unstable VTs were identified as those characterized by either (A) mean ABP during T_{VT} lower than 60 mmHg, i.e. $\overline{P_{VT}} < 60$ mmHg, where $\overline{P_{VT}} = mean_{t=T_{VT}}\,(x_{ABP}(t))$, with $x_{ABP}(t)$ representing continuous blood pressure, or by (B) a drop in mean ABP during VT higher than 30% from baseline mean ABP, i.e. $R^{TO}_{ABP} = \overline{P_{VT}}/\overline{P_{T0}} < 0.70$ or $R^{TSR}_{ABP} = \overline{P_{VT}}/\overline{P_{TSR}} < 0.7$, with baseline taken at T_0 and T_{SR}, respectively. These definitions are supported by previous studies and were adopted before data analysis [8], [9].

2) HEART RATE FROM ECG

The heart rate was estimated from the time-frequency (TF) distribution of the ECG waveform. The signal was down-sampled to 20 Hz and the TF spectrum was calculated using the quadratic distribution described in [10], [11]. The heart rate during T_0, T_{VT} and T_{SR} was measured as the temporal mean of the instantaneous frequencies, $f_0(t)$, identified as the highest spectral peak of the TF distribution. Only values above 40 bpm were considered as being valid heart rates.

3) PPG PARAMETERS

Five PPG metrics based on the PPG signal, $V(t)$, were defined to indirectly assess hemodynamics during VT. All of them

were expressed as the ratio between the metric's value during T_{VT} and baseline values obtained either during T_0 or T_{SR}.

1. R_A^{T0} and R_A^{TSR}: Ratio between the mean pulse amplitude during VT and baseline, where the pulse amplitude was measured from foot to peak for each pulse within T_{VT}, T_0 and T_{SR}.
2. R_{MS}^{T0} and R_{MS}^{TSR}: Ratio between the pulse maximum slope during VT and baseline. The pulse maximum slope was measured as the temporal mean of the maximum of the first derivative of each pulse: $\overline{V'_M} = \frac{1}{N} \cdot \sum_n V'_M[n]$, where $n = 1, \ldots, N$ is a heartbeat and $V'_M[n]$ is the maximum of the first derivative measured during the pulse's upslope, $V'_M = max\,(dV(t)/dt)$.
3. R_{MAS}^{T0} and R_{MAS}^{TSR}: Ratio between the mean absolute slope during VT and baseline. The mean absolute slope was measured as the temporal mean of the absolute value of the first derivative of the PPG signal, $\overline{|V'|} = mean_T \left| \frac{dV(t)}{dt} \right|$.
4. R_{PR}^{T0} and R_{PR}^{TSR}: Ratio between the pulse rate during VT and baseline. The pulse rate was measured as the barycentre of the power spectrum of $V(t)$ estimated using the Fourier transform of the PPG signal within the windows of interest T_{VT}, T_0 and T_{SR}.
5. R_{IP}^{T0} and R_{IP}^{TSR}: Ratio between the average instantaneous power of $V(t)$ during VT and baseline. The average instantaneous power was measured as $mean_T \left(\int_{f_0(t)-B_L}^{f_0(t)+B_H} S\,(t,f)df \right)$, where $f_0(t)$ is the instantaneous frequency of the highest spectral peak, $(B_L - B_H)$ are the boundaries of the time-varying spectral band where the instantaneous power is estimated and $S\,(t,f)$ is the TF distribution described in [10], [12]. B_L and B_H were set at ±10 bpm within baseline windows T_0 and T_{SR} and at -10 to +70 bpm within the VT window T_{VT}.

Of note, R_A and R_{MS} are the only metrics to require PPG peaks detection, which during some VTs can be challenging due to the loss of the pulsatile components in the PPG signal (see Fig. 1B).

4) SENSITIVITY ANALYSIS

Sensitivity analyses were conducted to assess the impact of choosing different thresholds for the definition of unstable VTs (see Section II.B1) and varying the duration of windows T_{VT}, T_0 and T_{SR} from 5 to 15 seconds.

C. STATISTICAL ANALYSIS

Distributions of data are presented as mean ± standard deviation, unless otherwise specified. Correlation between ABP and PPG parameters was measured using the Spearman's correlation coefficient. Differences between PPG and ECG parameters during hemodynamically stable vs unstable VTs were assessed using the Wilcoxon rank-sum test using a threshold for statistical significance equal to 0.05/N, where N = 23 represents the number of pair-wise comparisons (see Table 1).

TABLE 1.

(A)	$\overline{P_{VT}} < 60$	$\overline{P_{VT}} > 60$	P	cc
R_A^{T0}	0.55±0.25	0.71±0.15	**2.65E-04**	0.36
R_{MS}^{T0}	0.53±0.25	0.75±0.15	**3.42E-06**	0.54
R_{MAS}^{T0}	0.70±0.26	1.06±0.23	**2.36E-07**	0.57
R_{PR}^{T0}	0.49±0.35	0.80±0.30	**1.34E-04**	0.42
R_{IP}^{T0}	0.98±0.06	1.02±0.04	3.06E-03	0.30
R_A^{TSR}	0.49±0.22	0.70±0.13	**2.93E-06**	0.52
R_{MS}^{TSR}	0.51±0.28	0.77±0.16	**1.82E-06**	0.54
R_{MAS}^{TSR}	0.70±0.36	1.18±0.38	**9.04E-07**	0.52
R_{PR}^{TSR}	0.48±0.41	0.95±0.46	**1.62E-05**	0.48
R_{IP}^{TSR}	0.16±0.16	0.39±0.20	**7.26E-07**	0.58
HR_{VT}	155±25	132±24	**5.17E-04**	-0.45
(B1)	$R_{ABP}^{T0} < 0.7$	$R_{ABP}^{T0} > 0.7$	**P**	**cc**
R_A^{T0}	0.49±0.28	0.68±0.17	**6.79E-04**	0.44
R_{MS}^{T0}	0.43±0.17	0.72±0.19	**3.52E-06**	0.61
R_{MAS}^{T0}	0.61±0.25	0.99±0.26	**8.17E-06**	0.73
R_{PR}^{T0}	0.40±0.33	0.75±0.32	**3.18E-04**	0.55
R_{IP}^{T0}	0.96±0.07	1.01±0.04	8.97E-03	0.39
HR_{VT}	166±25	135±23	**7.43E-05**	-0.6
(B2)	$R_{ABP}^{TSR} < 0.7$	$R_{ABP}^{TSR} > 0.7$	**P**	**cc**
R_A^{TSR}	0.49±0.20	0.69±0.16	**5.43E-06**	0.52
R_{MS}^{TSR}	0.50±0.28	0.76±0.17	**1.30E-06**	0.62
R_{MAS}^{TSR}	0.64±0.31	1.19±0.37	**8.47E-09**	0.69
R_{PR}^{TSR}	0.43±0.37	0.97±0.45	**7.10E-07**	0.6
R_{IP}^{TSR}	0.14±0.13	0.39±0.20	**5.50E-08**	0.64
HR_{VT}	159±23	131±23	**1.30E-05**	-0.54

Mean and standard deviation of PPG and ECG parameters in hemodynamically stable and unstable VTs, P-value of their differences and correlation coefficients, cc, with invasive blood pressure parameters ($\overline{P_{VT}}$ in A, R_{ABP}^{T0}in B1 and R_{ABP}^{TSR} in B2). P<2.17E-03 (Bonferroni corrected threshold) are reported in bold.

Binary classification of stable and unstable VTs was assessed using receiver operating curves (ROC), from which the area under the curve (AUC), sensitivity and specificity were measured. For each parameter, the threshold providing best accuracy was defined as that associated with the ROC point closest to the upper left corner (Sensitivity = Specificity = 100%). Given that the number of events was relatively small (n = 75), AUC, sensitivity and specificity were first estimated using all events as both training and test set. However, to assess possible overestimation due to overfitting, classification assessment was then repeated by randomly splitting all events into a training test composed of 80% of events, and an independent test set composed of the remaining 20%. The optimum threshold was estimated from the training set and used to assess sensitivity and specificity in the independent test set. This process was repeated 10 times and results are reported as mean ± standard deviation.

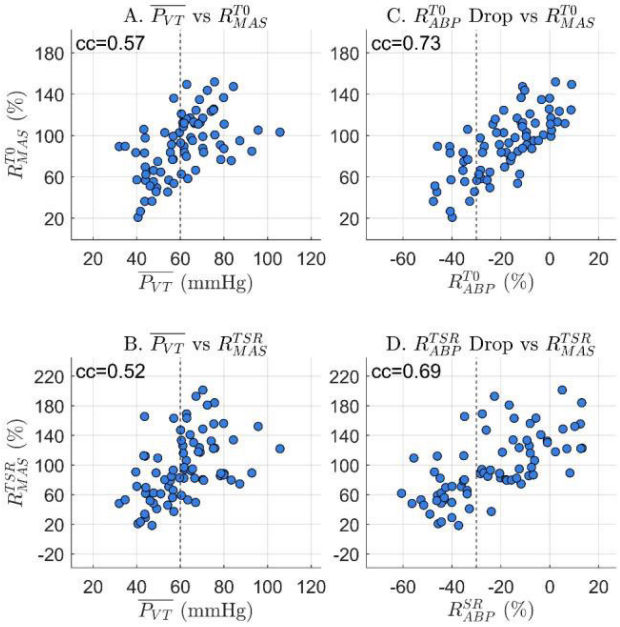

FIGURE 2. Correlation between invasive blood pressure (ABP) features (mean ABP during VT, $\overline{P_{VT}}$, ABP reduction during VT with respect to baseline, R^{T0}_{ABP} and R^{TSR}_{ABP}) and PPG features (ratio of mean absolute slope during VT with respect to baseline, R^{T0}_{MAS} and R^{TSR}_{MAS}). Correlation coefficient (cc) is shown within each panel.

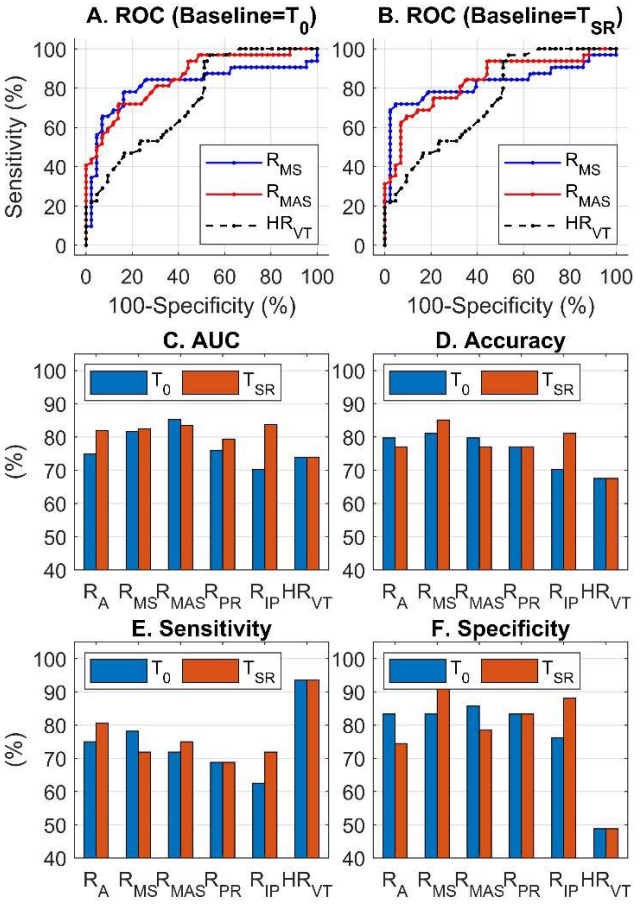

FIGURE 3. Classification of stable vs unstable VT based on mean blood pressure during the first 10 sec of VT. ROCs show classification results for the heart rate from the ECG (HR_{VT}) and 2 of the best PPG features (R_{MS} and R_{MAS}) using either T_0 (A) or T_{SR} (B) as baseline. Panels C-F show the area under the curve (AUC), accuracy, sensitivity and specificity for all features measured using T_0 (blue) or T_{SR} (red) as baseline.

Least absolute shrinkage and selection operator (LASSO) models were used to identify the best pair of features for classification. Logistic regressions utilizing the selected pair of parameters were used for classification and assessed as described before, i.e. both using all data for training and test and then using 80% of data for training and 20% for testing.

III. RESULTS

Fourteen patients exhibited at least one VT episode and a total of 75 VTs were analysed. Table 1 reports the distribution of parameters within stable and unstable VT groups, the P-value of their differences and the correlation coefficient between PPG and ABP parameters. Boxplots providing a graphical representation of these results are shown in Supplementary Fig. S.1-2. Fig. 2 illustrates the relation between ABP changes and PPG mean absolute slope for all VT episodes. Table 2 reports results of the binary classification including AUC, optimum threshold, accuracy, sensitivity and specificity estimated within the entire data-set and using separate training and test sets.

A. IDENTIFICATION OF UNSTABLE VT

VT episodes were classified as hemodynamically stable or unstable based on two criteria: A) Mean ABP during VT lower than 60 mmHg ($\overline{P_{VT}} < 60$ mmHg) and B) Drop of ABP larger than 30% with respect to baseline ($R^{T0}_{ABP} < 0.70$ or $R^{TSR}_{ABP} < 0.70$ if baseline was taken at T_0 or T_{SR}, respectively).

Thirty-two (n = 32, 42.7%) of VTs showed $\overline{P_{VT}} < 60$ mmHg. The heart rate was higher during unstable than stable VTs ($HR_{VT} = 155 \pm 25$ bpm vs 132 ± 24 bpm, $P = 5.2\ 10^{-4}$). All PPG parameters except R^{T0}_{IP} were significantly lower (P<2.17E-03) during unstable than stable VTs (see Table IIA). Among PPG parameters, R^{T0}_{MAS} and R^{TSR}_{MAS} showed the highest correlation with $\overline{P_{VT}}$, $cc = 0.57$ and $cc = 0.52$, respectively (Fig. 2A-B).

Classification of unstable VTs ($\overline{P_{VT}} < 60$ mmHg) using heart rate from the ECG was moderately accurate, with AUC = 0.74, high sensitivity (94%) but low specificity (49%). Classification was more accurate using PPG parameters, with R^{T0}_{MS} and R^{T0}_{MAS} providing the best results within parameters requiring and not-requiring PPG pulse detection, respectively. For these indices, AUC was >0.80 and accuracy was >80%, with specificity slightly higher than sensitivity. Results, including ROC curves, are summarized in Fig. 3.

Analysis performed using separate training and test data-sets showed similar results (Table 2 A).

Seventeen (n = 17, 23%) VTs showed $R^{T0}_{ABP} < 0.70$ and were considered hemodynamically unstable using this definition. As shown in Table IB, the heart rate correlated

TABLE 2. VT Classification using uni-variable models.

A. Mean ABP during VT < 60 mmHg

REF	PRED	SIG	PD	AUC	THR	ACC	SENS	SPEC	AUC	THR	ACC	SENS	SPEC
$\overline{P_{VT}} < 60$	R_A^{T0}	PPG	Y	75	0.63	80	75	83	74±2.6	0.63±0.00	85±9	84±13	86±9.8
$\overline{P_{VT}} < 60$	R_A^{TSR}	PPG	Y	82	0.62	77	81	74	82±1.7	0.61±0.02	71±10	72±29	67±13
$\overline{P_{VT}} < 60$	R_{MS}^{T0}	PPG	Y	82	0.65	81	78	83	81±1.5	0.65±0.02	80±6	79±16	80±14
$\overline{P_{VT}} < 60$	R_{MS}^{TSR}	PPG	Y	83	0.58	85	72	95	82±1.8	0.63±0.04	76±11	68±27	76±13
$\overline{P_{VT}} < 60$	R_{MAS}^{T0}	PPG	N	85	0.84	80	72	86	85±2.1	0.84±0.00	80±9.4	76±14	84±11
$\overline{P_{VT}} < 60$	R_{MAS}^{TSR}	PPG	N	84	0.86	77	75	79	83±1.8	0.84±0.03	75±6.7	76±15	74±10
$\overline{P_{VT}} < 60$	R_{PR}^{T0}	PPG	N	76	0.52	77	69	83	76±2.2	0.56±0.07	76±8	76±10	76±14
$\overline{P_{VT}} < 60$	R_{PR}^{TSR}	PPG	N	79	0.53	77	69	83	80±1.8	0.53±0.02	71±8.5	68±19	74±6.8
$\overline{P_{VT}} < 60$	R_{IP}^{T0}	PPG	N	78	0.52	77	72	81	80±3.1	0.49±0.03	76±8	63±21	87±12
$\overline{P_{VT}} < 60$	R_{IP}^{TSR}	PPG	N	84	0.18	81	72	88	84±1.7	0.19±0.01	77±10	72±17	79±12
$\overline{P_{VT}} < 60$	HR_{VT}	ECG	-	74	128	68	94	49	74±2.7	133±10	61±8.1	72±28	51±18

B. Drop of ABP > 30%

REF	PRED	SIG	PD	AUC	THR	ACC	SENS	SPEC	AUC	THR	ACC	SENS	SPEC
$R_{ABP}^{T0} < 0.7$	R_A^{T0}	PPG	Y	77	0.59	78	76	79	80±4.3	0.60±0.02	71±9.9	67±31	71±14
$R_{ABP}^{TSR} < 0.7$	R_A^{TSR}	PPG	Y	81	0.62	78	86	73	81±2.6	0.61±0.01	77±6.8	71±22	81±14
$R_{ABP}^{T0} < 0.7$	R_{MS}^{T0}	PPG	Y	87	0.57	82	82	82	87±1.9	0.58±0.02	77±7.4	80±29	75±11
$R_{ABP}^{TSR} < 0.7$	R_{MS}^{TSR}	PPG	Y	83	0.66	80	80	80	82±3.1	0.65±0.02	84±6.8	80±18	86±9.1
$R_{ABP}^{T0} < 0.7$	R_{MAS}^{T0}	PPG	N	86	0.84	77	82	75	86±2.1	0.84±0.00	76±9.5	70±24	77±11
$R_{ABP}^{TSR} < 0.7$	R_{MAS}^{TSR}	PPG	N	90	0.82	86	83	89	89±2.1	0.82±0.00	87±6.7	86±11	87±8.9
$R_{ABP}^{T0} < 0.7$	R_{PR}^{T0}	PPG	N	79	0.52	73	76	72	80±3.8	0.51±0.02	69±8.0	63±30	70±13
$R_{ABP}^{TSR} < 0.7$	R_{PR}^{TSR}	PPG	N	84	0.53	80	73	84	83±2.3	0.50±0.04	83±8.5	67±23	92±11
$R_{ABP}^{T0} < 0.7$	R_{IP}^{T0}	PPG	N	84	0.40	82	76	84	84±3.8	0.41±0.02	79±7.2	83±30	78±7
$R_{ABP}^{TSR} < 0.7$	R_{IP}^{TSR}	PPG	N	87	0.18	84	77	89	87±1.9	0.19±0.01	82±6.0	80±16	84±12
$R_{ABP}^{T0} < 0.7$	HR_{VT}	ECG	-	82	149	76	76	75	81±2.2	150±5.0	71±7.3	72±22	70±8.7
$R_{ABP}^{TSR} < 0.7$	HR_{VT}	ECG	-	80	149	77	67	84	80±1.8	148±1.7	71±9.3	63±10	78±15

Classification of hemodynamically unstable VTs based on its definition (REF) using the parameter (PRED); Results are obtained using all events for training and testing (left) or using 80% of events for training and 20% for testing (right, results reported as mean and standard deviation over 10 iterations). SIG: type of signal, either PPG or ECG; PD: Pulse detection required; AUC: Area under the ROC; THR: Threshold for best accuracy; ACC: Accuracy; SENS: Sensitivity; SPEC: Specificity.

only moderately to R_{ABP}^{T0} ($cc = 0.6$) and it was significantly higher in VTs characterized by sudden and significant ABP drop ($R_{ABP}^{T0} < 0.70$) than for the rest of VTs. All PPG parameters except R_{IP}^{T0} were significantly lower during VTs characterized by sudden and significant ABP drop than during the rest of VTs (Table 1B). R_{MAS}^{T0} showed the highest correlation coefficient with R_{ABP}^{T0} at cc = 0.73 (Table 1B). Classification was more accurate using PPG parameters than heart rate from the ECG, with R_{MS}^{T0} and R_{MAS}^{T0} providing the best results within parameters requiring and not-requiring PPG pulse detection, respectively. For these indices, AUC≥0.82 and accuracy was ≥77%, with similar specificity and sensitivity. Results, including ROC curves, are summarized in Supplementary Fig. S.3. Analysis performed using separate training and test data-sets or that used T_{SR} as baseline window showed similar results (Table 2B).

B. SENSITIVITY ANALYSES

Sensitivity analyses were conducted to explore how the use of different parameters affected the accuracy of stable vs unstable VT classification.

1) IMPACT OF ARBITRARY THRESHOLDS FOR UNSTABLE VTs

Data and statistical analysis were repeated for different thresholds, with unstable VTs identified as those for which $\overline{P_{VT}} < X$, with $50 < X < 70$ mmHg or R_{ABP}^{T0} and $R_{ABP}^{TSR} < X$, with $0.60 < X < 0.80$. Prevalence of unstable VT varied between 27% and 72% in the first case and between 11% and 56% in the second case. Fig. 4 shows AUC of HR_{VT}, R_{MAS} and R_{MS} as a function of the threshold used to identify unstable VTs based on mean ABP and ABP drop. AUC remained high for all configurations, and tended to slightly increase for thresholds that made unstable VT more severe

TABLE 3. VT Classification using lasso to identify the best pair of pre.

REF	PRED	AUC	ACC	SENS	SPEC	AUC	ACC	SENS	SPEC
$\overline{P_{VT}} < 60$	R^{T0}_{MAS}; HR_{VT}	87	84	84	84	86±2.0	83±7.2	83±15.9	86±8.4
$\overline{P_{VT}} < 60$	R^{TSR}_{MAS}; R^{TSR}_{A}	85	81	81	81	83±1.9	84±11.4	91±14.4	78±19.0
$R^{T0}_{ABP} < 0.7$	R^{T0}_{MAS}; R^{T0}_{MS}	89	83	82	83	88±2.3	82±8.3	84±21.7	82±11.6
$R^{TSR}_{ABP} < 0.7$	R^{TSR}_{MAS}; HR_{VT}	94	91	87	93	94±1.6	85±9.3	82±16.8	88±14.7

Results for the best 2-variables logistic regressions selected using the LASSO method. See Table II for details.

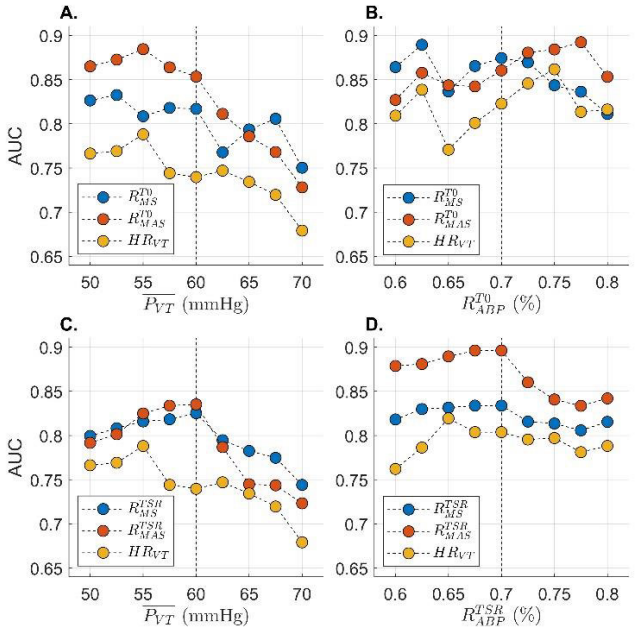

FIGURE 4. Classification using the heart rate from the ECG (HR_{VT}) and 2 of the best PPG features (R_{MS} and R_{MAS}) for different thresholds defining stable and unstable VTs based on invasive blood pressure. Panels show the area under the ROC (AUC) for unstable VTs defined by mean arterial blood pressure (ABP) lower than a threshold ranging from 50 to 70 mmHg, i.e. 50 $<\overline{P_{VT}}<$ 70 mmHg (A and C), and for a reduction of ABP during VT with respect to baseline windows T_0 (B) or T_{SR} (D) ranging from 60% to 80%, i.e. 60% $<R^{T0}_{ABP}<$ 80% and 60% $<R^{TSR}_{ABP}<$ 80%.

and less frequent (e.g. $\overline{P_{VT}} < 55$ mmHg). Of note, AUC remained higher for PPG markers R_{MAS} and R_{MS} than for heart rate in all configurations.

2) IMPACT OF USING DIFFERENT WINDOW LENGTHS

Data and statistical analysis were repeated after modifying the duration of T_{VT}, T_0 and T_{SR} from 5 s to 15 s. The results (Supplementary Tables S.II-III) show that this did not significantly impacted on the accuracy of stable and unstable VTs classification.

C. COMBINING PARAMETERS FOR MULTIPLE REGRESSIONS

The pairs of parameters providing the best classification of VTs showing $\overline{P_{VT}}< 60$, $R^{T0}_{ABP}< 0.7$ and $R^{TSR}_{ABP}< 0.7$ are shown in Table 3. In all cases, R_{MAS} was retained as one of the two best features. Classifications improved with respect to single-variable models, with AUC ranging from 0.85 for the detection of $\overline{P_{VT}}< 60$ mmHg using $\left(R^{TSR}_{MAS};R^{TSR}_{A}\right)$ to 0.94 for the detection of $R^{TSR}_{ABP}< 0.7$ using $\left(R^{TSR}_{MAS};HR_{VT}\right)$. Results obtained using a separate test sets confirmed high sensitivity and specificity for all multi-variables logistic regressions (Table 3).

IV. DISCUSSION

This study investigates for the first time the use of PPG markers to identify VTs characterized by hemodynamic compromise within 10 sec from its onset, a critical aspect for improving therapy in patients at risk of sudden cardiac death. The main findings are: (1) PPG markers can detect hemodynamically unstable VTs with accuracy as high as 86%; (2) Detection of unstable VTs was more accurate using PPG parameters than the heart rate measured from the ECG, independently of the specific ABP threshold or definition of unstable VTs. (3) The combination of PPG markers and heart rate improved accuracy, suggesting that PPG provides complementary information to the ECG. (4) Accurate pulse detection in the PPG is not necessary to accurately detect unstable VTs.

The hemodynamic response to VTs (i.e. stable vs unstable) was characterized both in terms of mean ABP and sudden changes in mean ABP. Results show that PPG parameters can detect both accurately. All PPG markers were expressed as a ratio between a given PPG feature measured during the first 10 sec of VT and during a baseline interval, which was defined either as the 10 sec preceding the VT onset independent of the heart rhythm (T_0), or as the earliest 10 sec of sinus rhythm preceding VT (T_{SR}). The rational for establishing this second baseline window was that VT is sometimes preceded by runs of ectopic beats. Additionally, in this study, some VTs were induced by ventricular pacing that can potentially affect both ABP and PPG. Results obtained using these different baseline windows were similar, which suggests that any interval preceding VT can serve as baseline, even in presence of irregular rhythm.

The heart rate measured during VT, which represents the standard parameter utilized to programme ICDs and prevent sudden cardiac death, was found to only moderately correlate with mean ABP ($cc = -0.45$) or sudden drop in mean ABP ($cc = -0.60$). While this is not surprising (ABP critically depends on cardiac function/contractility), it confirms the

need for a better estimator of the hemodynamic response to VT. The PPG parameter R_{MAS} showed the highest correlation with mean ABP ($cc = 0.57$) and sudden drop in mean ABP ($cc = 0.73$) during VT, and one of the best accuracy in classifying unstable and stable VTs (AUC$\leq$0.85). Furthermore, R_{MAS} is easy to estimate as it does not require PPG pulse detection. This makes it one of the most promising parameters for further clinical validation.

Previous studies have proposed algorithms to reduce false alarms in critical care [6], [13], with some of them including ventricular tachycardia. Another study has demonstrated high accuracy in discriminating between VT and ventricular fibrillation and between ICD shocked and non-shocked rhythms using features based on Taylor-Fourier analysis of the ECG [7]. The present study differs in many aspects as it focused for the first time on the challenge of non-invasively discriminating haemodynamically unstable VTs from haemodynamically stable VTs, it uses simultaneous invasive blood pressure recordings instead of surrogate parameters (e.g. ICD shocks) as a reference, and it focused on PPG features. Electromechanical coupling analysis has been recently used with success [14] to discriminate ventricular fibrillation from sinus rhythm or artefacts using used two laser doppler flowmetry light probes, one at the heart and the other at the finger. Compared to PPG, this laser doppler is a complex and expensive technology that uses coherent light to measure perfusion, which limits the application to in-clinic use.

In this study, we have focused on PPG, because, in contrast with cardiac signals such as the ECG, it offers an insight into hemodynamic cardiovascular changes. It functions by illuminating arterially perfused tissue within light in the visible and infra-red spectrum and recording the reflected tissue light. As an estimator of blood pressure, PPG has been limited by calibration requirements, and has been shown to perform well only in some patients [15], [16]. Interestingly, PPG had already been shown potential to detect hypotensive events during haemodialysis and labour [17], [18], but it was never been utilized to classify the hemodynamic response to VT. We have recently shown that PPG features can be used to detect mechanical (or pulsus) alternans [19], [20]. Combined with the present results, this suggests that although PPG may not be accurate in measuring ABP, it can be used to detect fast and sudden changes in ABP though the analysis of its pulsatile components.

A. CLINICAL RELEVANCE AND FUTURE APPLICATIONS

PPG sensors are commonly utilized for measuring oxygen saturation and are ubiquitous in clinics. In recent years, they have been increasingly incorporated in wearable health tracking devices (e.g. smart watches) that can provide a platform for improved individualized treatment. We envisage that future wearable/implanted devices could be used in combination with ICDs to enable a precise assessment of the hemodynamic response to VT, thus withholding unnecessary shock therapy and extending patient life expectancy. Combining ICD detected electrograms or surface ECG for rates below the standard VT zone rate cut-offs would also enable more accurate arrhythmia classification for determining therapy delivery in certain cases for slower VTs which can represent as significant challenge. Furthermore, PPG could be used to indirectly estimate respiratory rate [21]–[23], heart rate variability [24], mechanical alternans [19], [20] and other physiological markers to monitor cardiac risk and modulate ICD therapy (e.g. by preventively using anti-tachycardia pacing to prevent VTs). Cardiac risk assessment traditionally based on ECG parameters could be further benefit from the inclusion of ECG parameters. [25]–[28].

B. LIMITATIONS

The main limitation of the study was that data were recorded during electrophysiological studies. While this provides the unique opportunity to measure ABP, ECG and PPG during VT safely and in a controlled environment, the recording condition with the patients in supine position and the PPG measured at the finger with minimal movement differ from those in which the methodology is eventually intended to be used. Further study should address robustness against noise and movement artefacts. Furthermore, thresholds for obtaining the most accurate classification was performed by optimizing both sensitivity and specificity. While this is the standard approach, in a clinical scenario a high specificity at maximum sensitivity (no false negative) may be preferred. Finally, in this study the ECG was only used to derive the heart rate, because this is the standard parameter used to programme ICDs. Further studies may include ECG features derived with advanced methods [7].

V. CONCLUSION

This work has shown for the first time that PPG features can accurately classify hemodynamically stable and unstable VTs defined using simultaneous invasive recordings of arterial blood pressure. This may have potential clinical implications as reducing the number of unnecessary ICD shocks by specifically targeting unstable VT is a critical aspect of improving VT patients' care.

REFERENCES

[1] M. P. Turakhia, S. Zweibel, A. L. Swain, S. A. Mollenkopf, and M. R. Reynolds, "Healthcare utilization and expenditures associated with appropriate and inappropriate implantable defibrillator shocks," *Circulat., Cardiovascular Qual. Outcomes*, vol. 10, no. 2, Feb. 2017, Art. no. e002210, doi: 10.1161/CIRCOUTCOMES.115.002210.

[2] G. H. Bardy, K. L. Lee, D. B. Mark, and J. E. Poole, "Amiodarone or an implantable cardioverter–defibrillator for congestive heart failure," *New England J. Med.*, vol. 352, no. 3, pp. 225–237, Jan. 2005, doi: 10.1056/NEJMoa043399.

[3] D. J. Callans, J. Almendral, and M. E. Josephson, "Patients with hemodynamically tolerated ventricular tachycardia require implantable cardioverter-defibrillators," *Circulation*, vol. 116, no. 10, pp. 1196–1212, 2007, doi: 10.1161/CIRCULATIONAHA.106.670075.

[4] J. E. Poole, G. W. Johnson, A. S. Hellkamp, J. Anderson, D. J. Callans, M. H. Raitt, R. K. Reddy, F. E. Marchlinski, R. Yee, T. Guarnieri, M. Talajic, D. J. Wilber, D. P. Fishbein, D. L. Packer, D. B. Mark, K. L. Lee, and G. H. Bardy, "Prognostic importance of defibrillator shocks in patients with heart failure," *New England J. Med.*, vol. 359, no. 10, pp. 1009–1017, Sep. 2008, doi: 10.1056/NEJMoa071098.

[5] K. K. Steinbach, O. Merl, K. Frohner, and C. Hief, "Hemodynamics during ventricular tachyarrhythmias," *Amer. Heart J.*, vol. 127, no. 4, pp. 1102–1106, 1994, doi: 10.1016/0002-8703(94)90095-7.

[6] G. D. Clifford, I. Silva, B. Moody, Q. Li, D. Kella, A. Chahin, T. Kooistra, D. Perry, and R. G. Mark, "False alarm reduction in critical care," *Physiol. Meas.*, vol. 37, no. 8, pp. E5–E23, Aug. 2016, doi: 10.1088/0967-3334/37/8/E5.

[7] R. K. Tripathy, A. Zamora-Mendez, J. A. de la O Serna, M. R. A. Paternina, J. G. Arrieta, and G. R. Naik, "Detection of life threatening ventricular arrhythmia using digital Taylor Fourier transform," *Frontiers Physiol.*, vol. 9, p. 722, Jun. 2018, doi: 10.3389/fphys.2018.00722.

[8] F. Baratto, F. Pappalardo, T. Oloriz, C. Bisceglia, P. Vergara, J. Silberbauer, N. Albanese, M. Cireddu, G. D'Angelo, A. L. Di Prima, F. Monaco, G. Paglino, A. Radinovic, D. Regazzoli, S. Silvetti, N. Trevisi, A. Zangrillo, and P. Della Bella, "Extracorporeal membrane oxygenation for hemodynamic support of ventricular tachycardia ablation," *Circulat., Arrhythmia Electrophysiol.*, vol. 9, no. 12, Dec. 2016, doi: 10.1161/CIRCEP.116.004492.

[9] F. Lü, P. M. Eckman, K. K. Liao, I. Apostolidou, R. John, T. Chen, G. S. Das, G. S. Francis, H. Lei, R. G. Trohman, and D. G. Benditt, "Catheter ablation of hemodynamically unstable ventricular tachycardia with mechanical circulatory support," *Int. J. Cardiol.*, vol. 168, no. 4, pp. 3859–3865, Oct. 2013, doi: 10.1016/j.ijcard.2013.06.035.

[10] M. Orini, R. Bailon, L. T. Mainardi, P. Laguna, and P. Flandrin, "Characterization of dynamic interactions between cardiovascular signals by time-frequency coherence," *IEEE Trans. Biomed. Eng.*, vol. 59, no. 3, pp. 663–673, Mar. 2012, doi: 10.1109/TBME.2011.2171959.

[11] M. Orini, R. Bailón, P. Laguna, L. T. Mainardi, and R. Barbieri, "A multivariate time-frequency method to characterize the influence of respiration over heart period and arterial pressure," *EURASIP J. Adv. Signal Process.*, vol. 2012, no. 1, p. 214, Dec. 2012, doi: 10.1186/1687-6180-2012-214.

[12] M. Orini, E. Pueyo, P. Laguna, and R. Bailon, "A time-varying nonparametric methodology for assessing changes in QT variability unrelated to heart rate variability," *IEEE Trans. Biomed. Eng.*, vol. 65, no. 7, pp. 1443–1451, Jul. 2018, doi: 10.1109/TBME.2017.2758925.

[13] Q. Li and G. D. Clifford, "Signal quality and data fusion for false alarm reduction in the intensive care unit," *J. Electrocardiol.*, vol. 45, no. 6, pp. 596–603, Nov. 2012, doi: 10.1016/j.jelectrocard.2012.07.015.

[14] D. Keene, M. J. Shun-Shin, A. D. Arnold, J. P. Howard, D. Lefroy, D. W. Davies, P. B. Lim, F. S. Ng, M. Koa-Wing, N. A. Qureshi, N. W. F. Linton, J. S. Shah, N. S. Peters, P. Kanagaratnam, D. P. Francis, and Z. I. Whinnett, "Quantification of electromechanical coupling to prevent inappropriate implantable cardioverter-defibrillator shocks," *JACC: Clin. Electrophysiol.*, vol. 5, no. 6, pp. 705–715, Jun. 2019, doi: 10.1016/j.jacep.2019.01.025.

[15] H. Gesche, D. Grosskurth, G. Küchler, and A. Patzak, "Continuous blood pressure measurement by using the pulse transit time: Comparison to a cuff-based method," *Eur. J. Appl. Physiol.*, vol. 112, no. 1, pp. 309–315, Jan. 2012, doi: 10.1007/s00421-011-1983-3.

[16] A.-G. Pielmuş, D. Osterland, M. Klum, T. Tigges, A. Feldheiser, O. Hunsicker, and R. Orglmeister, "Correlation of arterial blood pressure to synchronous piezo, impedance and photoplethysmographic signal features," *Current Directions Biomed. Eng.*, vol. 3, no. 2, pp. 749–753, Sep. 2017, doi: 10.1515/cdbme-2017-0158.

[17] J. Bolea, J. Lázaro, E. Gil, E. Rovira, J. M. Remartínez, P. Laguna, E. Pueyo, A. Navarro, and R. Bailón, "Pulse rate and transit time analysis to predict hypotension events after spinal anesthesia during programmed cesarean labor," *Ann. Biomed. Eng.*, vol. 45, no. 9, pp. 2253–2263, Sep. 2017, doi: 10.1007/s10439-017-1864-y.

[18] F. Sandberg, R. Bailón, D. Hernando, P. Laguna, J. P. Martínez, K. Solem, and L. Sörnmo, "Prediction of hypotension in hemodialysis patients," *Physiol. Meas.*, vol. 35, no. 9, pp. 1885–1898, Sep. 2014, doi: 10.1088/0967-3334/35/9/1885.

[19] T. Besleaga, S. Badiani, G. Lloyd, N. Toschi, A. Canichella, A. Demosthenous, P. D. Lambiase, and M. Orini, "Non-invasive detection of mechanical alternans utilizing photoplethysmography," *IEEE J. Biomed. Health Informat.*, vol. 23, no. 6, pp. 2409–2416, Nov. 2019, doi: 10.1109/JBHI.2018.2882550.

[20] S. van Duijvenboden, B. Hanson, N. Child, P. D. Lambiase, C. A. Rinaldi, G. Jaswinder, P. Taggart, and M. Orini, "Pulse arrival time and pulse interval as accurate markers to detect mechanical alternans," *Ann. Biomed. Eng.*, vol. 47, no. 5, pp. 1291–1299, May 2019, doi: 10.1007/s10439-019-02221-4.

[21] A. Garde, P. Dehkordi, W. Karlen, D. Wensley, J. M. Ansermino, and G. A. Dumont, "Development of a screening tool for sleep disordered breathing in children using the phone Oximeter," *PLoS ONE*, vol. 9, no. 11, Nov. 2014, Art. no. e112959, doi: 10.1371/journal.pone.0112959.

[22] D. Álvarez, A. Crespo, F. Vaquerizo-Villar, G. C. Gutiérrez-Tobal, A. Cerezo-Hernández, V. Barroso-García, J. M. A., G. A. Dumont, R. Hornero, F. del Campo, and A. Garde, "Symbolic dynamics to enhance diagnostic ability of portable oximetry from the phone oximeter in the detection of paediatric sleep apnoea," *Physiol. Meas.*, vol. 39, no. 10, Oct. 2018, Art. no. 104002, doi: 10.1088/1361-6579/aae2a8.

[23] M. D. Peláez-Coca, M. Orini, J. Lázaro, R. Bailón, and E. Gil, "Cross time-frequency analysis for combining information of several sources: Application to estimation of spontaneous respiratory rate from photoplethysmography," *Comput. Math. Methods Med.*, vol. 2013, pp. 1–8, 2013, doi: 10.1155/2013/631978.

[24] E. Gil, M. Orini, R. Bailón, J. M. Vergara, L. Mainardi, and P. Laguna, "Photoplethysmography pulse rate variability as a surrogate measurement of heart rate variability during non-stationary conditions," *Physiol. Meas.*, vol. 31, no. 9, pp. 1271–1290, Sep. 2010, doi: 10.1088/0967-3334/31/9/015.

[25] M. Orini, B. Hanson, V. Monasterio, J. P. Martinez, M. Hayward, P. Taggart, and P. Lambiase, "Comparative evaluation of methodologies for T-Wave alternans mapping in electrograms," *IEEE Trans. Biomed. Eng.*, vol. 61, no. 2, pp. 308–316, Feb. 2014, doi: 10.1109/TBME.2013.2289304.

[26] J. Ramírez, M. Orini, A. Mincholé, V. Monasterio, I. Cygankiewicz, A. Bayés de Luna, J. P. Martínez, P. Laguna, and E. Pueyo, "Sudden cardiac death and pump failure death prediction in chronic heart failure by combining ECG and clinical markers in an integrated risk model," *PLoS ONE*, vol. 12, no. 10, Oct. 2017, Art. no. e0186152, doi: 10.1371/journal.pone.0186152.

[27] J. Ramírez, M. Orini, and A. Mincholé, "T-wave morphology restitution predicts sudden cardiac death in patients with chronic heart failure," *J. Amer. Heart Assoc.*, vol. 6, no. 5, May 2017, Art. no. e005310, doi: 10.1161/JAHA.116.005310.

[28] J. Ramirez, M. Orini, J. D. Tucker, E. Pueyo, and P. Laguna, "Variability of ventricular repolarization dispersion quantified by time-warping the morphology of the T-Waves," *IEEE Trans. Biomed. Eng.*, vol. 64, no. 7, pp. 1619–1630, Jul. 2017, doi: 10.1109/TBME.2016.2614899.

TUDOR BESLEAGA was born in Bucharest, Romania, in 1991. He received the M.Eng. degree in mechanical engineering with business finance and the M.Res. degree in medical device innovation from University College London, London, U.K., in 2014 and 2015, respectively, where he is currently pursuing the Ph.D. degree in biomedical engineering.

PIER D. LAMBIASE graduated from Oxford University, in 1992, and received the Ph.D. degree from King's College London, in 2003. He is currently a Professor of cardiology at University College London and the Barts Heart Centre. His research is focused on mechanisms of inherited and acquired heart rhythm disorders.

ADAM J. GRAHAM received the M.B.B.S. degree from St Bartholomew's Hospital and the London Medical School, in 2008. He had a membership with the Royal College of Medicine, in 2011. He is currently a Fellow of electrophysiology at the Barts Heart Centre.

ANDREAS DEMOSTHENOUS (Fellow, IEEE) received the B.Eng. degree in electrical and electronic engineering from the University of Leicester, Leicester, U.K., in 1992, the M.Sc. degree in telecommunications technology from Aston University, Birmingham, U.K., in 1994, and the Ph.D. degree in electronic and electrical engineering from University College London (UCL), London, U.K., in 1998.

He is currently a Professor at the Department of Electronic and Electrical Engineering, UCL, and leads the Analog and Biomedical Electronics Group. He has made outstanding contributions to improving safety and performance in integrated circuit design for active medical devices, such as spinal cord and brain stimulators. He has numerous collaborations for cross-disciplinary research, both within the U.K. and internationally. He has authored over 300 articles in journals and international conference proceedings, several book chapters, and holds several patents. His research interests include analog and mixed-signal integrated circuits for biomedical, sensor, and signal processing applications. He is a Fellow of the Institution of Engineering and Technology and a Chartered Engineer. He was a co-recipient of a number of best paper awards and has graduated many Ph.D. students. He has served on the technical committees for a number of international conferences, including the European Solid-State Circuits Conference (ESSCIRC) and the International Symposium on Circuits and Systems (ISCAS). He was an Associate Editor, from 2006 to 2007, and the Deputy Editor-in-Chief, from 2014 to 2015, of the IEEE TRANSACTIONS ON CIRCUITS AND SYSTEMS II: EXPRESS BRIEFS, and an Associate Editor, from 2008 to 2009, and the Editor-in-Chief, from 2016 to 2019, of the IEEE TRANSACTIONS ON CIRCUITS AND SYSTEMS I: REGULAR PAPERS. He is an Associate Editor of the IEEE TRANSACTIONS ON BIOMEDICAL CIRCUITS AND SYSTEMS and serves on the International Advisory Board of *Physiological Measurement*.

MICHELE ORINI received the M.Sc. degree in biomedical engineering from the Politecnico di Milano, Italy, the M.Eng. degree from the École Centrale Paris, France, in 2006, and the joint Ph.D. degree from the University of Zaragoza, Spain, and the Politecnico di Milano, Italy, in 2012. He is currently a Senior Research Fellow at University College London, where he has made important contributions to data science applied to the understanding and treatment of cardiovascular disease.